

CDK2-dependent activation of PARP-1 is required for hormonal gene regulation in breast cancer cells

Roni H.G. Wright,¹ Giancarlo Castellano,¹ Jaume Bonet,² Francois Le Dily,¹ Jofre Font-Mateu,¹ Cecilia Ballaré,¹ A. Silvina Nacht,¹ Daniel Soronellas,¹ Baldo Oliva,² and Miguel Beato^{1,3}

¹Centre de Regulació Genòmica (CRG), Barcelona E-08003, Spain; ²Structural Bioinformatics Laboratory (SBI), Universitat Pompeu Fabra (UPF), Barcelona E-08003, Spain

Eukaryotic gene regulation implies that transcription factors gain access to genomic information via poorly understood processes involving activation and targeting of kinases, histone-modifying enzymes, and chromatin remodelers to chromatin. Here we report that progestin gene regulation in breast cancer cells requires a rapid and transient increase in poly-(ADP)-ribose (PAR), accompanied by a dramatic decrease of cellular NAD that could have broad implications in cell physiology. This rapid increase in nuclear PARylation is mediated by activation of PAR polymerase PARP-1 as a result of phosphorylation by cyclin-dependent kinase CDK2. Hormone-dependent phosphorylation of PARP-1 within the catalytic domain, enhances its enzymatic capabilities. Activated PARP-1 contributes to the displacement of histone H1 and is essential for regulation of the majority of hormone-responsive genes and for the effect of progestins on cell cycle progression. Both global chromatin immunoprecipitation (ChIP) coupled with deep sequencing (ChIP-seq) and gene expression analysis show a strong overlap between PARP-1 and CDK2. Thus, progestin gene regulation involves a novel signaling pathway that connects CDK2-dependent activation of PARP-1 with histone H1 displacement. Given the multiplicity of PARP targets, this new pathway could be used for the pharmacological management of breast cancer.

[*Keywords:* mouse mammary tumor virus; progesterone receptor; transcriptional regulation; histone H1; PARP-1; chromatin remodeling]

Supplemental material is available for this article.

Received March 30, 2012; revised version accepted July 11, 2012.

Eukaryotic gene regulation requires that transcription factors gain access to genomic information via processes involving activation and targeting of kinases, histone-modifying enzymes, and chromatin remodelers to chromatin. Post-translational modification of chromatin and chromatin-modifying enzymes is a key component of gene regulation mechanisms; however, in this context, one such modification, poly-(ADP)-ribosylation (PARylation) catalyzed by the PAR polymerase (PARP) family of enzymes, remains poorly characterized (Chambon et al. 1963; Ame et al. 2004). PARP-1 and PAR play a role in regulating chromatin structure in various physiological contexts and after DNA damage, as PARylation of histones destabilizes nucleosomes (Poirier et al. 1982; Kraus and Lis 2003). Although PARP-1 was identified as the transcription factor TFIIC (Slattery et al. 1983), its activation and role in transcriptional regulation in the absence of DNA

damage remained unclear (Tulin et al. 2002; Kraus and Lis 2003; Kim et al. 2004; Parvi et al. 2005). Here we report that progestin gene regulation and subsequent cell proliferation in breast cancer cells require a rapid and transient increase in PAR, mediated by activation of PARP-1. PARP-1 activation is the result of phosphorylation by the hormone-activated cyclin-dependent kinase CDK2 at two consecutive serine residues, leading to enhanced PARylation capabilities. As PARP-1 is required for ligand-induced transcriptional activation following 17 β estradiol and retinoic acid treatment (Parvi et al. 2005; Ju et al. 2006) and interacts with progesterone receptor (PR) (Sartorius et al. 2000), we demonstrate the mechanism of PARP-1 activation in breast cancer cells. PARP-1 activation contributes to displacement of histone H1, an essential step for regulation of the majority of hormone-responsive genes and for the effect of progestins on cell cycle progression. Both global chromatin immunoprecipitation (ChIP) coupled with deep sequencing (ChIP-seq) and gene expression analysis show a strong overlap between PARP-1 and CDK2. Thus, progestin gene regulation involves a novel signaling pathway

³Corresponding author

E-mail miguel.beato@crg.es

Article is online at <http://www.genesdev.org/cgi/doi/10.1101/gad.193193.112>.

connecting CDK2-dependent activation of PARP-1 with histone H1 displacement, offering a potential target for endocrine control of breast cancer progression.

Results

PAR levels dramatically increase following hormone treatment

First, we estimated the levels of PAR and PARP-1 by immunofluorescence at different time points after hormone treatment of T47D-MTVL (T47D^M) breast cancer cells that carry a single integrated copy of a luciferase transgene driven by the mouse mammary tumor virus (MMTV) promoter (Truss et al. 1995). Nuclear PAR levels increased dramatically after treatment with the synthetic progesterone analog R5020 for 15 min (Fig. 1A, left panel). Levels of PAR markedly increased 5 min following hormone addition, remained high for 30 min, and returned to basal values after 60 min (Fig. 1B, top panel). The increase in PAR and PARylated proteins following hormone treatment was blocked by the PARP inhibitor 3AB (Fig. 1B, top panel, dashed line; Supplemental Fig. S1A). Concomitantly with the increase in PAR, the levels of PARP substrate NAD dropped after progestin treatment (Fig. 1B, bottom panel). The decrease in NAD levels was due to PARP activity, as it was abrogated by 3AB (Fig. 1B, bottom panel, dashed line). Thus, breast cancer cells respond to progestin treatment with a rapid and transient increase in PARylation of nuclear proteins catalyzed by the hormonal activation of members of the PARP family.

Activation of PARP plays a role in induction of the progesterone reporter gene in T47D^M cells. The 14-fold increase in MMTV-luc transcription observed after 6 h of hormone treatment was significantly compromised following prior incubation with PARP inhibitor 3AB in a dose-dependent manner (Supplemental Fig. S1B). Similar results were observed with the PARP inhibitors PJ34 and NAP (Supplemental Fig. S1C). To date, 17 PARP family members have been identified, although PARP-1 is responsible for ~90% of PAR formed in cells (Ame et al. 2004). To confirm that PARP-1 is indeed the PARP responsible for the increase in PAR levels observed following hormone treatment, we generated T47D^M cells depleted of PARP-1 by stable expression of a specific shRNA (Fig. 1C). We observed no phenotypic or growth abnormalities (Supplemental Fig. S2A,B) in PARP-1 knockdown cell lines; however, we did observe that the hormonal activation of the MMTV transgene was reduced by >70% compared with control shRNA cell lines (Fig. 1D). In addition, the induction of endogenous progesterone target genes *c-Fos*, *DUSP1*, and *EGFR* was also significantly reduced in the PARP-1 knockdown cell lines (Fig. 1E). Treatment of T47D^M cells with progestin induces a single round of proliferation, and this progestin-induced proliferation of T47D^M cells was compromised in the absence of PARP-1 (Fig. 1F; Supplemental Fig. S2D); therefore, we conclude that gene induction and activation of cell proliferation by progestin depend on PARylation and an increase in PARP-1 activity.

CDK2 activates PARP-1 in response to hormone treatment

To test whether activation of PARP-1 is mediated by one of the hormone-activated kinases, we measured the effect of several kinase inhibitors on the formation of PAR after progestin treatment (Supplemental Table S1). Only Cdk2i, an inhibitor of CDK2, significantly ($P < 0.05$) abrogated the levels of PAR following hormone treatment (Supplemental Fig. S3A). Notably, inhibitors of the damage kinases ATM and ATR did not inhibit hormone-dependent PAR accumulation, suggesting a distinct signaling cascade from that activated during DNA damage. CDK2 is rapidly activated by progesterone in T47D^M cells and plays an important role in hormone gene regulation (Lange 2008; Vicent et al. 2011).

To confirm that CDK2 is involved in hormonal activation of PARP-1, CDK2 was knocked down in T47D^M cells using specific siRNA. Depletion of CDK2 compromised the hormone-induced PAR accumulation, as determined by either Western blotting or ELISA (Fig. 2A [cf. lanes 3 and 4], B, respectively). Thus, the increase in PAR levels observed as quickly as 5 min following hormone treatment is dependent on CDK2 activity. The observed decrease in cellular NAD levels following hormone treatment was also inhibited by the inhibition of CDK2 (Supplemental Fig. S3B).

CDK2 in complex with Cyclin A and PR is required for the activation of some progesterone target genes (Narayanan et al. 2005; Vicent et al. 2011). Therefore, we tested whether genes dependent on PARP-1 activity are similarly affected by inhibition of CDK2. Hormonal induction of the MMTV-*luc* transgene—in addition to endogenous genes *c-Fos*, *DUSP1*, and *EGFR*—was markedly inhibited in the presence of the CDK2 inhibitor (Fig. 2C,D, respectively). Hormonal PARP-1 activation could be direct, since PARP-1 and CDK2 specifically interact following hormone treatment (Fig. 2E), suggesting that PARP-1 is a direct target of hormone-activated CDK2. Interaction studies using HA-CDK2 truncations revealed a region of CDK2 between amino acids 150 and 200, comprising the second cyclin-binding domain (CBD), as responsible for the interaction with PARP-1 (Fig. 2F). The use of GST-PARP-1 proteins revealed that the CDK2 interaction domain of PARP-1 resides within the automodification domain encompassing the BRCA1 C-terminal (BRCT) domain (amino acids 326–525), a known protein–protein interaction domain for other PARP-1-binding partners, including PARP2, DNA ligase III (Schreiber et al. 2002), XRCC1 (Masson et al. 1998), DNA Pol β (Dantzer et al. 2000), histones, and transcription factors *Oct1* and YY1 (Fig. 2G; Oei and Shi 2001).

CDK2 phosphorylates PARP-1, resulting in a more catalytically active enzyme

PARP-1 is phosphorylated by CDK2 in vitro (Fig. 3A), and sequential in vitro phosphorylation and PARylation assays demonstrated that phosphorylated PARP-1 had a higher auto-PARylation activity as compared with unphosphorylated PARP-1 (Fig. 3B, cf. lanes 1 and 3). The

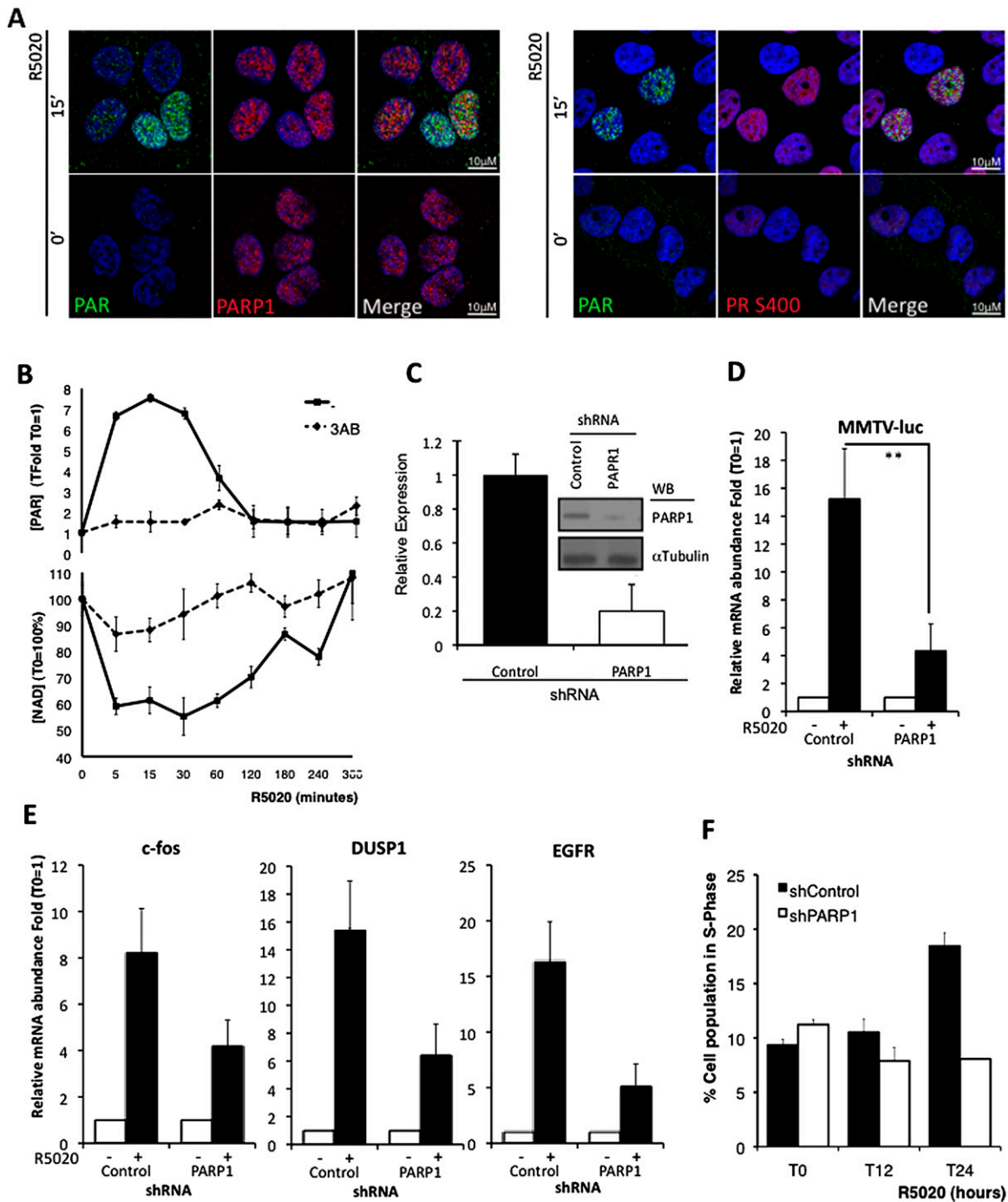


Figure 1. PAR rapidly accumulates following progestin stimulation. (A) PAR levels (green) increase in T47D^M cells treated with R5020 for 15 min. Levels of PARP-1 (left panels) and phosphorylated PR Ser400 (right panels), as a measure of cells responding to R5020, are shown in red. Bar, 10 μ m. (B) Elevation in PAR levels (solid line), as measured by PAR-capture ELISA following R5020, is inhibited by 3AB (dashed line); hormone causes a concomitant decrease in cellular NAD levels (solid line, bottom panel), which is also 3AB-dependent (dashed line, bottom panel). (C) PARP-1 knockdown by specific shRNA was confirmed by mRNA expression (histogram) and Western blotting (inset). R5020 induced higher mRNA levels from the MMTV-luc transgene (D) as well as from *c-fos*, *DUSP1*, and *EGFR* (E), all of which are abrogated in PARP-1 knockdown cell lines. (***) $P < 0.01$. Error bars represent the SEM. (F) The percentage of the cell population residing in S phase 24 h following R5020 was determined in PARP-1 knockdown and control cell lines.

trans-PARylation of histone H1 was also enhanced by prior phosphorylation of PARP-1 by CDK2 (Fig. 3B, cf. lanes 2 and 4). This enhancement of PARylation is not merely

stabilized by the CDK2–PARP-1 interaction. It needs enzymatic activity, demonstrated by a kinase-dead CDK2, which is unable to enhance PARylation (Supplemental

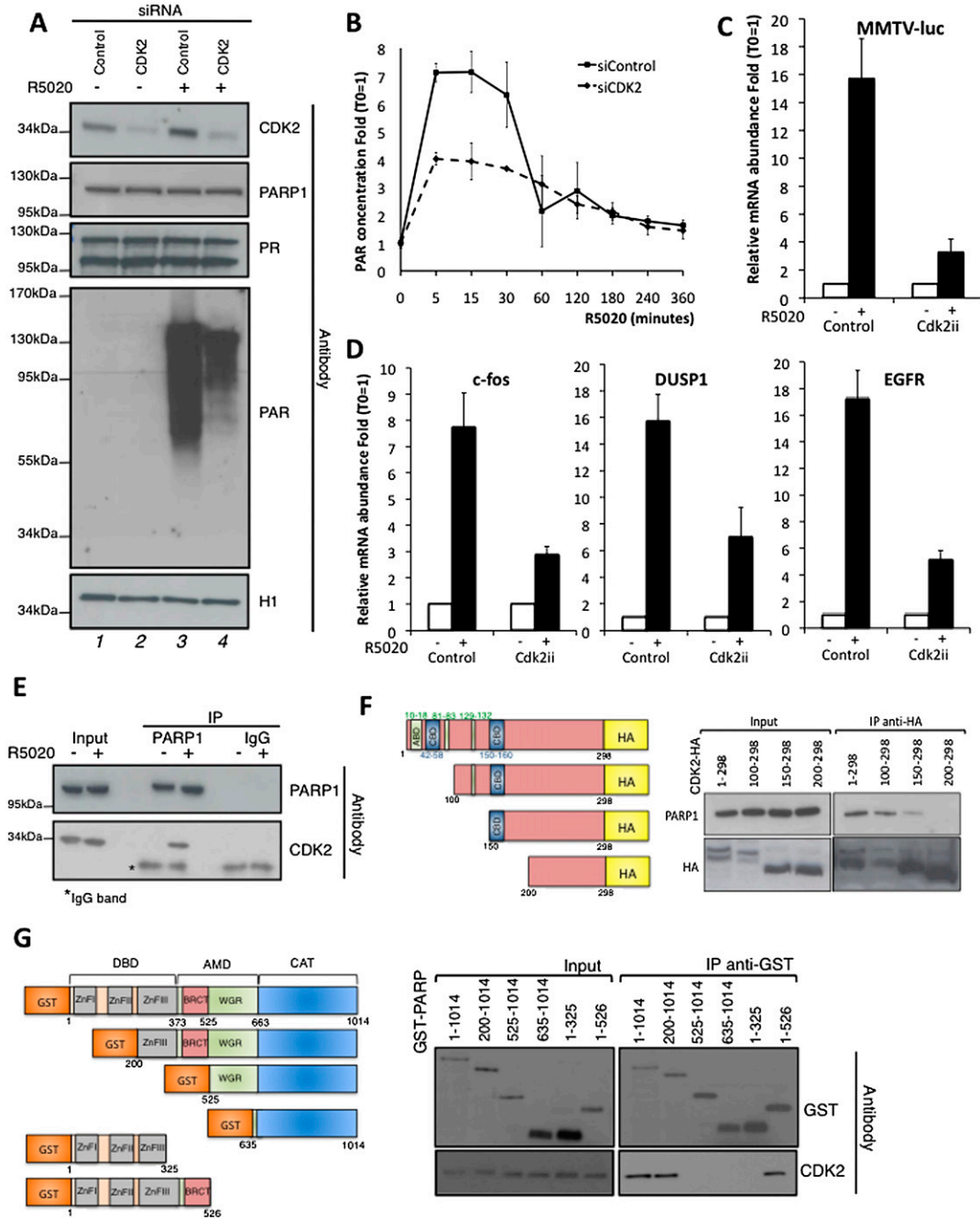


Figure 2. CDK2 is needed for PARP activation and hormonal activation. T47D^M cell lysates transfected with either control or CDK2 siRNA for 48 h were harvested following incubation with R5020 for 15 min (+). (A) The elevation in PAR levels following R5020 is dependent on CDK2 as determined by Western blotting using CDK2- and PAR-specific antibodies. Levels of PARP-1 and PR proteins are given as controls. (B) The increase in PAR levels, as measured by PAR-capture ELISA in T47D^M cells treated with R5020 over time, is inhibited in T47D^M cells treated with CDK2-specific siRNA compared with cells transfected with control siRNA. Error bars represent the SEM. Increased mRNA expression of the MMTV-luc transgene (C) as well as *c-fos*, *DUSP1*, and *EGFR* (D) in response to R5020 is dependent on CDK2 enzymatic activity, as the CDK inhibitor Cdk2ii blocks it. Error bars represent the SEM. (E) Immunoblot showing the hormone-dependent interaction of endogenous PARP-1 and CDK2 in T47D^M cells treated with R5020 (+) for 30 min using PARP-1- and CDK2-specific antibodies. (*) A nonspecific IgG band. (F) CDK2 interacts with PARP-1 via amino acids 150–200 partially encompassing the second CBD. (Left diagram) T47D^M cells were transfected for 48 h with plasmids encoding HA-CDK2 truncations ([ABD] ATP-binding domain; numbers correspond to amino acid number). (Right panel) Cell extracts were prepared, immunoprecipitated using anti-HA-specific antibody, and probed for the interaction with PARP-1 by Western blotting. (G) PARP-1 interacts with CDK2 via the automodification domain encompassing the BRCT domain (amino acids 325–526). (Left diagram) Purified GST-PARP-1 truncation proteins ([ZnF]zinc finger; [BRCT] BRCT domain; [DBD] DNA-binding domain [AMD]; automodification domain; [CAT] catalytic domain; numbers correspond to amino acid number), purified from bacteria, were incubated with recombinant CDK2 for 2 h prior to incubation with GST beads. (Right) The interaction of GST-PARP-1 mutants with CDK2 was determined by Western blotting using GST- and CDK2-specific antibodies.

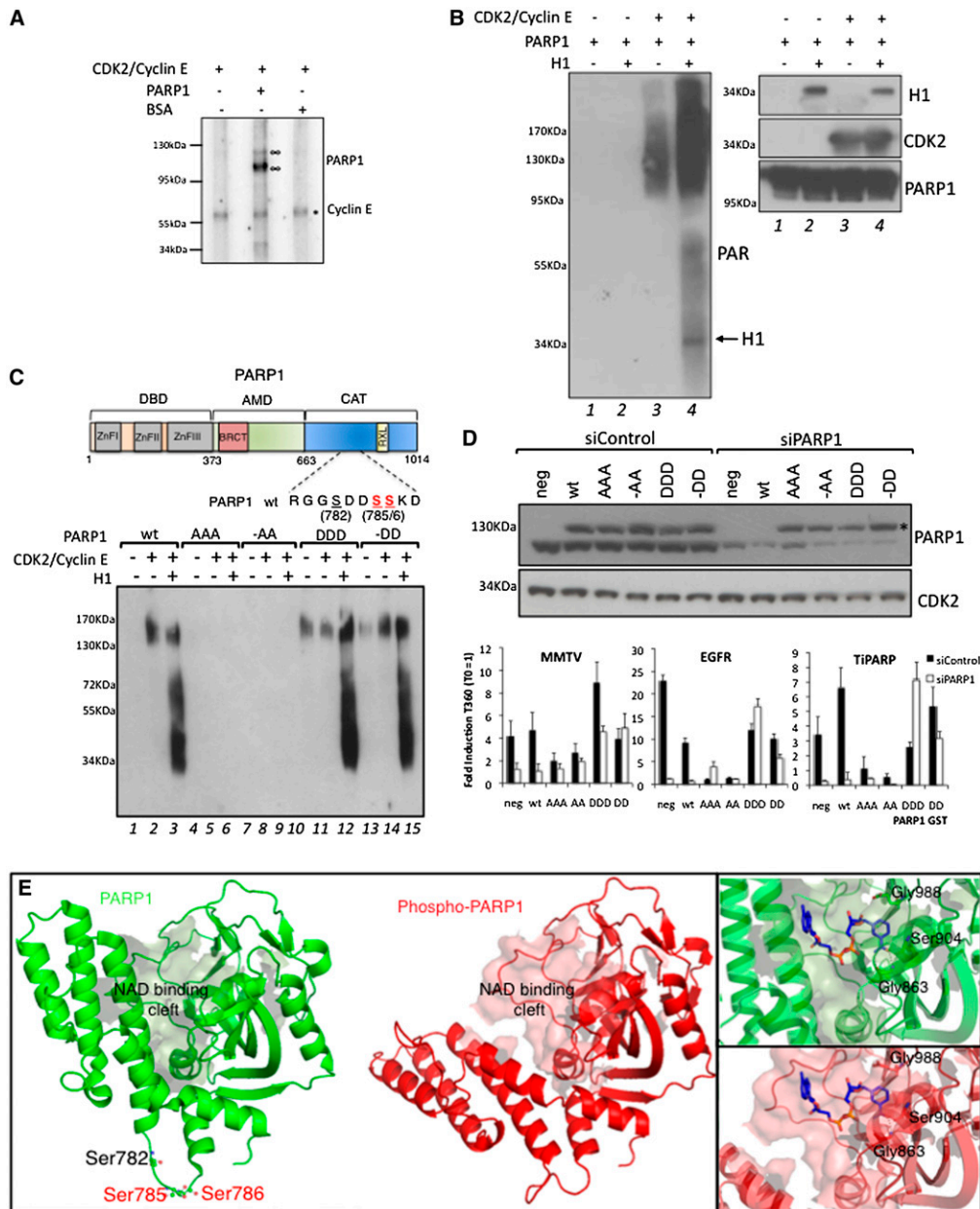


Figure 3. CDK2 phosphorylates PARP-1 in vitro and in vivo, leading to increased enzyme activity and predicted changes in the active site. (A) Recombinant CDK2 phosphorylates recombinant PARP-1 in vitro using g[p32]ATP as substrate, as visualized by SDS-gel electrophoresis and autoradiogram. (∞) Phosphorylated PARP-1; (*) phosphorylated Cyclin E as internal control. (B) CDK2 phosphorylation of PARP-1 enhances its auto- and *trans*-ADP-ribosylation activity as determined by sequential phosphorylation (in the presence or absence of CDK2/Cyclin E) and PARylation (in the presence or absence of H1) assays. (Left panel) Levels of PAR produced were determined by Western blot using a PAR-specific antibody (PARylation of H1 is indicated by an arrow). The right panel shows a Western blot as control for the levels of the added proteins. (C) The diagram indicates the locations of the hormone-induced CDK2-dependent (red) or CDK2-independent (black) PARP-1 phosphorylation sites and the cyclin-binding RXL domain. GST-PARP-1 mutants were expressed and purified from T47D^M cells (Supplemental Fig. S5D,E). The ability of CDK2 to enhance the PARylation activity of GST-PARP-1 phospho-null mutants (PARP-1 AAA/-AA; lanes 4-9) is significantly reduced compared with wild-type (wt) GST-PARP-1 (lanes 1-3), in contrast to the constitutively active PARylation capabilities observed using GST-PARP-1 phosphomimetic mutants (lanes 10-15), as determined by in vitro PARylation followed by immunoblot against PAR. (D, top panel) The protein levels of both endogenous PARP-1 and GST-PARP-1 (*) following cotransfection of siRNA (either control or PARP-1-specific) and plasmids encoding GST-PARP-1 si-resistant mutants in T47D^M cell lines were determined by Western blotting using PARP-1 antibody. CDK2 levels are shown as a loading control. (Bottom panel) Phosphomimetic, but not phospho-null mutations of PARP-1 are able to rescue hormone-induced gene response following PARP-1 knockdown. Hormone induction of the MMTV-luc transgene, EGFR, and TiPARP 6 h following hormone treatment in T47D^M cell lines cotransfected with control siRNA (black bars) or PARP-1 siRNA (white bars) and GST-PARP-1 si-resistant rescue plasmids as described above. Values are given as a fold change over T0 = 1. (E) The opening of the catalytic domain due to the conformational change predicted by phosphorylation is clearly visible comparing the predicted structure of the unphosphorylated (green) or phosphorylated (red) PARP-1 catalytic domains. The right panels highlight residues Gly988, Ser904, and Gly863, essential for NAD (ligand shown) binding, residing within the NAD-binding cleft (amino acids 859-908 surface representation), which are not adversely affected by the shift in the catalytic domain induced by PARP-1 phosphorylation.

Fig. S4B), although it interacts with PARP-1 (Supplemental Fig. S4C). Thus, phosphorylation of PARP-1 by CDK2 and not solely the interaction between these two proteins is essential for PARP-1 activation.

To test whether hormone-dependent CDK2-mediated PARP-1 phosphorylation occurs *in vivo*, PARP-1 from control T47D^M cells or from cells treated with R5020 with or without prior incubation with the inhibitor Cdk2ii (Supplemental Fig. S5A) was analyzed by mass spectrometry. No significant phospho-peptides were found in the control sample, while three phospho sites were identified after hormone treatment, corresponding to Ser782, Ser785, and Ser786 of PARP-1. In cells treated with the CDK2 inhibitor, only the previously identified phospho site Ser782 (Mayya et al. 2009) was detected, suggesting that Ser785 and Ser786 are hormone-induced phospho sites dependent on CDK2 (Fig. 3C). PARP-1 contains a potential RXL domain (Supplemental Fig S5B) commonly found in CDK substrates facilitating proper substrate orientation and recognition by binding to the cyclin partner of the CDK (Adams et al. 1996). The phosphorylation of PARP-1 at Ser782, Ser785, and Ser786 by CDK2 is essential for the enhanced activity of PARP-1, as GST-PARP-1 Ser/Ala mutants greatly reduced the CDK2-enhanced activation of PARP-1 auto- and *trans*-PARylation capabilities (Fig. 3C, cf. lanes 1–3 and 4–9). In contrast, phosphomimetic mutation of these sites (Ser/Asp) gave rise to a constitutively active PARP-1, the activity of which is not enhanced further by CDK2 phosphorylation (Fig. 3C, cf. lanes 1–3 and 13–15; Supplemental Fig. 5E). The PARylation capabilities of PARP1 782 phospho-null (A-) and phosphomimetic (D-) mutants showed no significant changes (data not shown). As shown by PARP-1 being required for progesterone induction of target genes (Fig. 1E), overexpression of phospho-null PARP-1 mutants acted as dominant-negative, inhibiting the progesterone induction of target genes (Fig. 3D, black bars). Knockdown of PARP-1 resulted in impaired hormone induction (Fig. 3D, white bars), rescued by the addition of the si-resistant phosphomimetic PARP-1 but not the phospho-null mutants (Fig. 3D), confirming that the phosphorylation of PARP-1 is essential for the activation of downstream target genes.

We next asked whether this enhanced activity could be due to a structural change in the catalytic domain of PARP-1 induced by phosphorylation. The structure of the PARP-1 catalytic domain (Protein Data Bank [PDB] 3L3M) (Penning et al. 2005) was modeled mimicking phosphorylation at Ser782, Ser785, and Ser786 and revealed that the increase in negative charge results in the formation of a 3:10 helix (Lee et al. 2000), giving rise to a more open catalytic domain (Fig. 3E). This structural change significantly increases the exposition of the NAD acceptor site (Fig. 3E, surface representation) without affecting either the residues essential for NAD binding (Glu988, Ser904, or Gly863) (Fig. 3E, right panel) or the structural stability of the catalytic domain as a whole (Supplemental Fig. S6), thus supporting the hypothesis that phosphorylated PARP-1 is more catalytically active.

Hormone-induced gene regulation depends on both CDK2 and PARP-1 on a global scale

To obtain a global view of PARP-1 and CDK2 dependence in progesterone gene regulation, we performed gene expression microarrays with T47D^M cells untreated and treated with the progestin R5020 in the presence or absence of the PARP inhibitor 3AB or the CDK2 inhibitor Cdk2ii. We focused on the combined data set, which represents the genes that are significantly up-regulated or down-regulated in both arrays (Fig. 4A,B, Venn diagram). Eighteen percent of the genes in the combined list are dependent on CDK2 alone, and 12% depend on PARP exclusively. Only 15% of progestin-regulated genes in the combined list were independent of these two enzymes, while 85% (3219 genes in the combined data set) depended on either PARP-1 or CDK2 activity, with the majority (55%) depending on both. A heat map representation (Fig. 4A) and correlation analysis (Supplemental Fig. S7C) clearly show that induced or repressed genes are also affected in a similar manner and to a similar extent by both inhibitors ($R = 0.69$). A similar pattern of PARP-1 and CDK2 dependence is found comparing up-regulated genes or down-regulated genes (Fig. 4C). Gene-specific mRNA determinations by RT-PCR were used to validate this dependence on the enzymatic activities of both CDK2 and PARP-1 and confirmed the array results (Fig. 4D). Consistent with progesterone-induced cellular proliferation, pathway analysis of PARP- and CDK2-dependent gene lists showed an enrichment of MAPK signaling and cancer pathways (Supplemental Table S3). Gene ontology (GO) term biological functional analysis was consistent with previous reports showing an enrichment of stress, transcription, cell signaling (intracellular signaling cascades, kinase cascades, and enzyme-linked receptor signaling), cell proliferation, and metabolic functions (Supplemental Tables S4–S7).

As previously published (Vicent et al. 2011), we detected recruitment of PR and CDK2 to the MMTV nucleosome B as early as 1 min after hormone induction (Fig. 5A). Since histone H1 is one of the main targets of PARP-1 and displacement of histone H1 is one of the initial steps in hormone-responsive promoters (Vicent et al. 2011), we measured H1 loading by ChIP. We confirmed that histone H1 is displaced from the MMTV promoter already 1 min after hormone treatment (Fig. 5A) and remains low until 30 min (Supplemental Fig. S8A). The concomitant recruitment of PARP-1 and CDK2 and H1 displacement were confirmed at other progesterone-binding sites (PRBs) (Fig. 5B, right panel). As it has been reported that PARP-1 and histone H1 are mutually exclusive at gene promoters (Krishnakumar et al. 2008), we performed a ChIP assay in PARP-1 knockdown cell lines. PARP-1 enzymatic activity is not essential for the initial recruitment of PARP1 or PR to target promoters, as depletion of PARP-1 protein (shRNA) or enzymatic activity (3AB) did not abrogate recruitment of PR to the MMTV promoter (Fig. 5C; Supplemental Fig. 8A, respectively). In marked contrast, the displacement of histone H1 is dependent on PARP-1 activity and hence PARylation, as hormone-induced H1

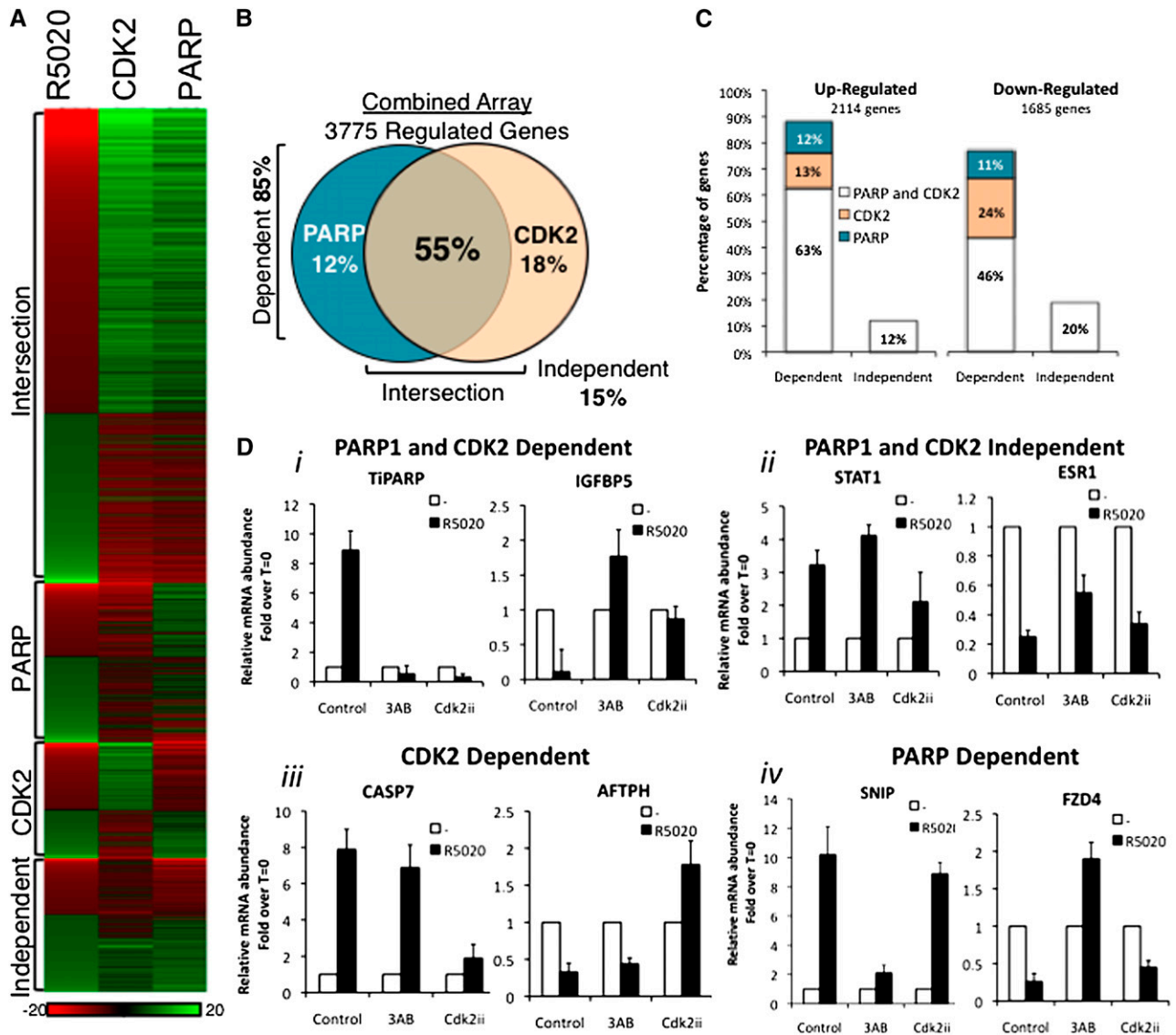


Figure 4. Global analysis of PARP-1 and CDK2 dependence of progesterin gene regulation. (A) The 3775 progesterin-regulated genes representing the combined PARP-1 and CDK2 arrays correlate in their response to the inhibitors, as visualized by a heat map. (The color code in the samples treated with inhibitors reflects the changes relative to the sample treated only with R5020.) Summary of the individual inhibitor arrays (Supplemental Fig. S7A,B). (B) Venn diagram of progesterin-regulated genes (bold; percentage of genes), indicating the dependence on CDK2 (18%), PARP-1 (12%), or both CDK2 and PARP-1 (intersection 55%), or independent of the two enzymes (15%). (C) Up-regulated and down-regulated progesterin-dependent genes are similarly affected by the inhibition of PARP-1 and CDK2. (D, panel *i*) mRNA expression levels of CDK2- and PARP-1-dependent genes *TIPARP* and *IGFBP5* was determined by quantitative RT-PCR (qRT-PCR) in cells treated with R5020 for 6 h in the presence or absence of 3AB or CDK2ii. (Panel *ii*) mRNA expression levels of CDK2- and PARP-1-independent genes *STAT1* and *ESR1* was determined by qRT-PCR in cells treated with R5020 for 6 h in the presence or absence of 3AB or CDK2ii. (Panel *iii*) mRNA expression levels of CDK2-dependent genes *CASP7* and *AFTPH* were determined by qRT-PCR in cells treated with R5020 for 6 h in the presence or absence of 3AB or CDK2ii. (Panel *iv*) mRNA expression levels of PARP-1-dependent genes *SNIP* and *FZD4* were determined by qRT-PCR in cells treated with R5020 for 6 h in the presence or absence of 3AB or CDK2ii (mean fold induction over T0 \pm SEM).

removal is blocked in PARP-1-depleted cell lines (Fig. 5C, cf. lanes 1–4 and 5–8) and in cells treated with 3AB (Supplemental Fig. S8A). We confirmed by re-ChIP experiments that following hormone treatment, binding of PARP-1 and CDK2 takes place on the same promoter (Fig. 5D). Moreover, hormone-dependent recruitment of PARP-1 and CDK2 as well as H1 displacement were

dependent on the catalytic activities of both enzymes, as they were blocked by prior treatment of T47D^M cells with either 3AB or Cdk2ii (Supplemental Fig. 8B). ChIP-seq analysis with antibodies to PARP-1 and CDK2 was performed at 0, 5, and 30 min following R5020, and a few thousand new peaks were found after hormone treatment (Fig. 5E, table), showing a significant corecruitment of

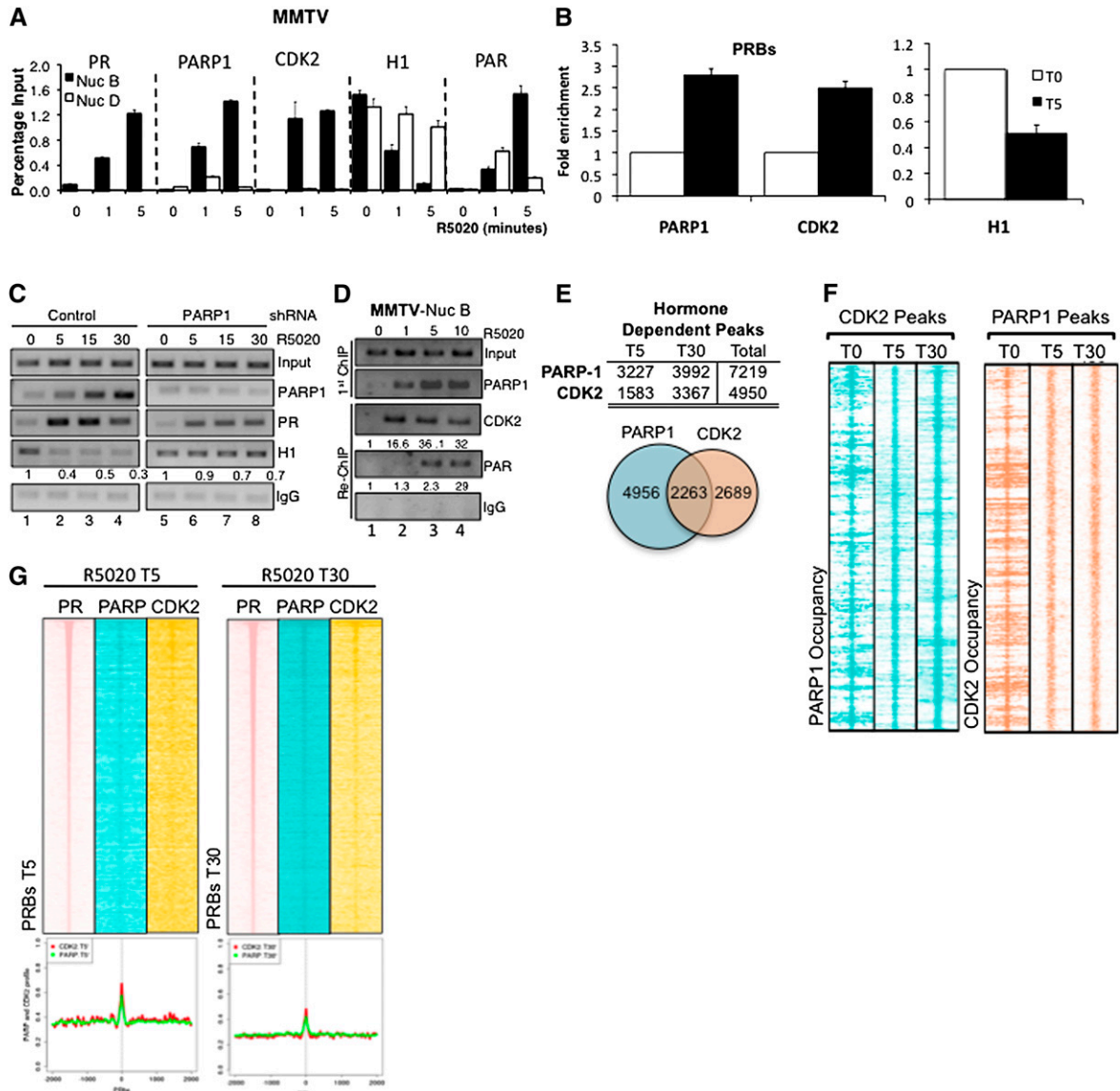


Figure 5. Global corecruitment of PARP-1 and CDK2 to chromatin and H1 displacement. (A) The recruitment of PR, PARP-1, CDK2, and PAR specifically to the MMTV nucleosome B (Nuc B) and not nucleosome D (Nuc D) following R5020 treatment and the concomitant H1 displacement is shown by ChIP RT-qPCR at the indicated time points after hormone treatment. (B) ChIP RT-qPCR shows the mean recruitment of PARP-1 and CDK2 in conjunction with H1 displacement following hormone treatment for 5 min to five different PR-binding sites. Error bars represent the SEM. (C) ChIP analysis in control or PARP-1 knockdown T47D^M cells at different times following R5020 treatment demonstrates that R5020-induced H1 displacement from MMTV nucleosome B is dependent on PARP-1 enzymatic activity; compare lanes 1–4 and 5–8. The values below the H1 row show the H1 content relative to the 0 time point. (D) Re-ChIP: PARP-1-immunoprecipitated material used for a second immunoprecipitation with CDK2 or PAR antibodies confirmed co-occupancy of PARP and CDK2 as well as PARP and PAR on MMTV nucleosome B following R5020 treatment. RT-qPCR quantification is shown below the panels. (E) The total number (table) and overlap/co-occupancy of both PARP-1 and CDK2 peaks identified following hormone treatment at T5 and T30 min (Venn diagram). (F) The chromatin occupancy of PARP-1 and CDK2 following hormone treatment significantly overlap. (Left) Raw sequencing tag distribution of PARP-1 in a region (± 2000 bp) centered on CDK2 peaks detected at 0, 5, and 30 min after hormone. (Right) Raw sequencing tag distribution of CDK2 in a region (± 2000 base pairs [bp]) centered on PARP-1 peaks detected at 0, 5, and 30 min after hormone treatment. (G) Heat map visualization of raw sequencing tag distribution of PR, PARP-1, and CDK2 at 5 min (left panel) and 30 min (right panel) after hormone treatment (R5020) in a region (± 2000 bp) flanking PRBs. The PRBs are sorted according to their number of sequence tags in descending order. A quantitative profile of both PARP-1 and CDK2 distribution is shown below the heat maps.

both proteins (Fig. 5E, Venn diagram). Globally, for both PARP-1 and CDK2, we observed peaks recruited and maintained at 5 and 30 min following hormone treatment

(Supplemental Fig. 9). Visualization of PARP-1 occupancy on chromatin specifically on a 2-kb region surrounding the CDK2 hormone-dependent peaks showed that PARP-1

is enriched within these regions (Fig. 5F, left panel). Further supporting the cooperation of these two enzymes, CDK2 occupancy is also enriched on chromatin in regions surrounding PARP-1 hormone-dependent peaks (Fig. 5F, right panel). Both CDK2 and PARP1 were enriched around PR-binding sites, supporting a role of PR in recruiting these proteins to progestin-regulated regions (Fig. 5G).

Discussion

In recent years, a DNA damage-independent role for PARP-1 in both the activation and repression of transcription has emerged (Kraus and Lis 2003; Luo and Kraus 2012), which can or cannot require PARP-1 enzymatic activity (Hassa et al. 2003; Ju et al. 2004; Cohen-Armon et al. 2007). Several lines of evidence link PARP-1 with nuclear receptor (NR)-mediated transcription. PARP-1 inhibition has been shown to block estrogen receptor α (ER α)-, androgen receptor (AR)-, retinoic acid receptor (RAR)-, and thyroid hormone receptor (T₃R)-dependent gene activation (Ju et al. 2006), but the role of PARP-1 in progesterone gene regulation has not been reported. Here we show that PARP-1 enzymatic activity is rapidly enhanced after progestin treatment of breast cancer cells and provide a molecular mechanism for this effect; namely, phosphorylation by hormone-activated CDK2. PARP-1 activation leads to a global increase in PAR levels that is essential for the induction or repression of the majority of progesterone-regulated genes. These findings differ from previous results by Parvi et al. (2005) showing that RAR-mediated transcription requires PARP-1, which, independent of its catalytic activity, converts Mediator from the inactive to the active state. Although Mediator and CDK2 both bind the BRCT domain of PARP-1, in progestin-treated breast cancer cells, the outcome is PARP-1 phosphorylation and enhancement of its enzymatic activity, likely by opening the NAD-binding cleft of its catalytic domain. Additional experiments will be needed to explore whether activated PARP1 also has an effect on the Mediator state in progestin-treated breast cancer cells.

Kinase-induced activation of PARP-1 in the absence of DNA damage was demonstrated previously to be essential for expression of Elk1 target genes and for promoting cell proliferation (Cohen-Armon et al. 2007). In contrast with a previous study (Inbar-Rozensal et al. 2009), we observed that although PARP-1 is not essential for breast cancer cell growth in response to serum factors, it is indispensable for progesterone-induced cell proliferation after serum starvation. This effect of PARP-1 on hormonal response seems to be specific for PR, since ER α and PARP1 do not interact, and PR and PARP-1 expression levels positively correlate in proliferative lesions, whereas the levels of ER and PARP-1 do not (Ghabreau et al. 2004).

Although both PARP-1 and CDK2 have been previously implicated in the transcription of hormone-regulated genes (Parvi et al. 2005; Ju and Rosenfeld 2006; Moore and Weigel 2011; Vicent et al. 2011), the molecular mechanism of PARP-1 activation and the pathway connecting these two enzymes had not been established. Our results identify a new signaling pathway going from

activated PR to activated CDK2 and PARP-1. Recently, the possibility of post-translational modification of PARP-1 mediating its activation has received considerable attention. Gagné et al. (2009) used a broad proteomic screen to identify several potential PARP-1 phosphorylation sites, including Ser372 and the residues Ser782/Ser785 and Ser786 identified here. Subsequent biochemical studies have confirmed that phosphorylation of S372 and Thr373 by ERK1/2 enhances PARP-1 activation following DNA damage (Kauppinen et al. 2006). We provide evidence showing that in the absence of DNA damage, phosphorylation at Ser785 and Ser786 by CDK2 enhances PARP-1 activation in response to progesterone. The role of phosphatases in PARP-1 control is of potential interest, as the increase in PAR levels induced by progesterone is a transient event.

In addition to elucidating the molecular basis of hormonal PARP1 activation, we also provide a possible mechanism for the role of PARP1 in gene regulation. Both PARP-1 and CDK2 are recruited to the large majority of progestin target genes, where they cooperate in displacement of the linker histone H1. We showed previously that H1 displacement is the first step in progestin-mediated gene regulation and that NURF and CDK2/Cyclin E participate in this process, which takes place within 1 min after hormone addition (Vicent et al. 2011). We now show that the PARylation activity of PARP-1 is also required for the displacement of histone H1. Highly negatively charged PAR covalently attached to target proteins has the potential to alter protein-protein interactions and biochemical activities as well as the retention of proteins in the chromatin environment (Luo and Kraus 2012). As we observed a transient increase in PAR, the precise role of PAR hydrolysis by PAR glycohydrolase (PARG) to free either PAR or mono(ADP-ribose) will be of particular interest in the future.

We propose the following model (Fig. 6): (1) PARP-1 and CDK2/Cyclin E interact following progestin stimulation. (2) This interaction, via the BRCT domain of PARP-1 and the CBD of CDK2, facilitates the phosphorylation of PARP-1 at S785/S786. (3) Phosphorylation of PARP-1 results in a more open NAD-binding pocket within the catalytic domain, enhancing PARP-1 activity, leading to autophosphorylation. (4) PARP-1 and CDK2/Cyclin E are corecruited to chromatin, resulting in PARylation of chromatin proteins and chromatin opening via the displacement of histone H1. (5) The cooperation between CDK2 and PARP-1 is indispensable for regulation of many progestin target genes, as inhibition of PARP-1 and/or CDK2 blocks the downstream activation or repression of 85% of progestin target genes.

This study provides further insight into previous findings proposing a role for PARP-1 activation in signaling pathways required for downstream chromatin modification and gene regulation in the absence of DNA damage. Given the multiplicity of known PARP interactors in conjunction with the wide array of potential PARylation targets, it remains to be explored whether PARP-1 fulfills other functions in gene regulation and whether knowledge of this new pathway can be used for the

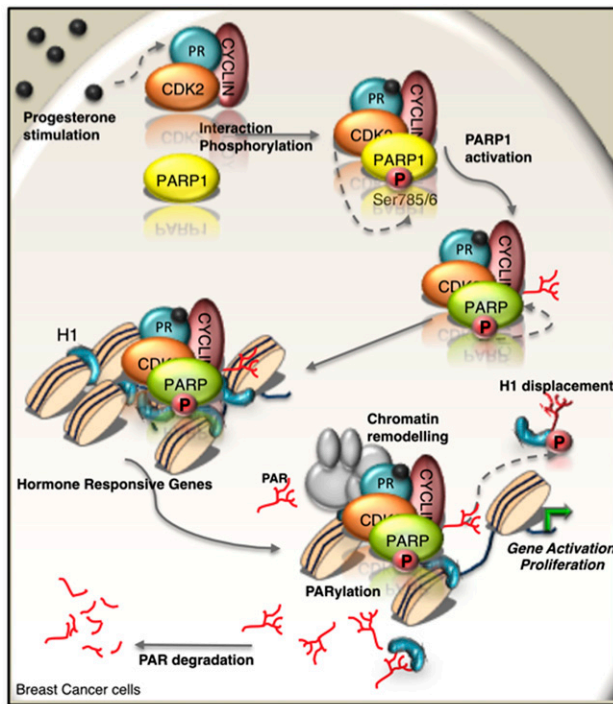


Figure 6. Model of progestin-induced PARP-1 activation by CDK2. PARP-1 activation via phosphorylation (S785/786) by CDK2 results in a more open catalytic domain and higher enzyme activity. This leads to a global increase in PAR levels, displacement of histone H1, and a more open chromatin environment, facilitating the recruitment of chromatin remodellers and transcriptional regulators essential for the induction or repression of the majority of progesterone-regulated genes.

pharmacological management of breast cancer (Inbar-Rozensal et al.2009).

Materials and methods

Cell culture

T47D^M cells were used for all experiments unless otherwise stated. For hormone induction experiments, cells were grown in RPMI medium without Phenol Red, supplemented with 10% dextran-coated charcoal-treated FBS (DCC/FBS) after 24 h in serum-free conditions; cells were incubated with R5020 (10 nM) or vehicle (ethanol) as described (Vicent et al. 2011). Inhibitor concentration and duration are given in Supplemental Table S1.

PAR purification

PAR was purified essentially as described (Aboul-Ela et al. 1988). Briefly, 5×10^6 human embryonic kidney (HEK) 293T cells were grown to confluency in 150-mm plates. The growth medium was removed, and the cells were exposed to 200 J/m² UVB irradiation. The medium was replaced, and 30 min later, the cells were harvested with trypsin. The resultant cell pellet was washed twice with PBS and precipitated with 20% final volume TCA. Following centrifugation at 1800g for 10 min at 4°C, pellets were washed with 20% TCA and twice with 100% ethanol and air-dried. The pellets were resuspended in 1 M KOH and 50 mM EDTA and vortexed to mix. Extracts were then incubated for 2 h

at 60°C with gentle agitation. A DHBB column was equilibrated with AAGE9 buffer (250 mM ammonium acetate at pH 9.0, 6 M guanine HCl). Samples were passed through the column twice, and the column was then washed with AAGE9 buffer before a final wash of 1 M ammonium acetate (pH 9.0). PAR was eluted from the resin with water, lyophilized overnight, and stored at -80°C until required.

In vitro PARylation assay

Unless otherwise indicated, the standard reaction contained 500 µg of wild-type PARP-1 (Trevigen) or 1 µg of GST-PARP-1 phosphomutants purified from mammalian cells previously phosphorylated in vitro by CDK2 as described (Supplemental Material). One-hundred micrograms of histone H1 (Millipore) and 200 ng of activated DNA were incubated in PARP-1 reaction buffer (400 µM NAD, 50 mM Tris-HEPES at pH 8.0, 0.15 mM KCl, 10 mM MgCl₂) for 30 min at 25°C. The reactions were stopped by the addition of 4× SDS loading buffer and analyzed on SDS-PAGE and Western blot probing for the presence of PAR using PAR-specific antibodies.

PAR-capture ELISA

Hormone and inhibitor treatments (Supplemental Table S1) were carried out as described, and sample preparation was carried out as follows: At the required time point, cells were washed twice with ice-cold PBS and scraped in lysis buffer (0.4 M NaCl, 1% Triton X-100) plus protease inhibitors. Cell suspensions were then incubated for 30 min on ice with periodic vortexing. The disrupted cell suspension was centrifuged at 10,000g for 10 min at 4°C, and the supernatant was recovered, snap-frozen, and stored at -80°C until required. Ninety-six-well black-walled plates were incubated with 2 ng/µL anti-PAR monoclonal antibody (Trevigen) in 50 mM sodium carbonate (pH 7.6) overnight at 4°C. The plates were washed once with PBS and blocked with blocking solution (5% semiskimmed milk powder, 0.1% Tween 20, 25 mM Tris at pH 7.4, 150 mM NaCl) for 1 h at room temperature. The plate was then washed four times in PBS and 0.1% Tween 20. One-hundred microliters of each sample (20 µg of total protein) or a PAR standard was applied and incubated for 1.5 h at room temperature. The plate was washed four times with PBS and 0.1% Tween 20 and incubated with anti-PAR rabbit polyclonal antibody (Trevigen) for 1.5 h at room temperature. The plate was washed four times with PBS and 0.1% Tween 20 and incubated with anti-rabbit HRP conjugate secondary antibody (5% semiskimmed dried milk) for 1.5 h at room temperature. The plate was washed six times with PBS and 0.1% Tween 20, and PAR was identified via incubation with TACs Sapphire (Trevigen) for 10 min in the dark. The reaction was terminated with 5% phosphoric acid, and the absorbance at 450 nm and 520 nm was recorded.

NAD depletion assay

T47D^M cells were either left untreated or treated with the inhibitor indicated (Supplemental Table S1) prior to R5020 addition as described. NAD concentration was determined as described (Jacobson and Jacobson 1976). At $T = t$, cells were washed with ice-cold PBS and incubated in 0.5 M PCA for 20 min on ice. An equal volume of KOH (1 M)/K₂HPO₄ (0.33 M) (pH 7.0) was added, and the samples were vortexed and incubated for 20 min on ice. Samples were spun at 10,000 rpm for 2 min at 4°C, and the supernatant was stored at -20°C. The quantification of NAD was carried out as follows: Samples were added to an equal volume of reaction buffer (200 mM Bicine at pH 7.8, 1 mg/mL

BSA, 1 M EtOH, 10 mM EDTA at pH 8.0, 4 mM phenazine). One-tenth of the reaction volume of alcohol dehydrogenase was added and incubated for 30 min at 30°C. The reaction was terminated with a 0.3× sample volume of 12 mM iodoacetate, and the absorbance at 570 nm was measured.

Purification of HA-CDK2 proteins for in vitro PARylation assays

HEK 293T cells were transfected with pCMV-neo-CDK2 HAwt (Addgene plasmid depository 1884) or pCMV-neo-CDK2HA_{dn} (Addgene plasmid depository 1885). Cells were serially diluted, and positive clones were selected with G418 (1 mg/mL). Expression of CDK2-HAwt or CDK2-HA_{dn} was confirmed by Western blot as described using HA-specific antibody (Abcam). Purification of CDK2-HA proteins was carried out under nondenaturing conditions as follows: Cell lysates from 6×10^6 cells were prepared and incubated with 100 μ L of prewashed anti-HA agarose slurry (Pierce, Thermo Scientific). Samples were incubated overnight at 4°C with gentle end-over-end mixing on a rocking platform. Agarose beads were washed three times with TBS-Tween 20 (0.05%) prior to HA-protein elution using 1 mg/mL HA-peptide (Pierce, Thermo Scientific) for 15 min at 30°C.

Generation of HA-CDK2 truncations for PARP-1 interaction studies

CDK2 truncations, including the HA tag (Fig. 2F) PCR-amplified from pCMV-neo-CDK2-HA (Addgene plasmid depository 1884), were subcloned using BamHI into empty pCMV-neo. PCR primers are available on request. The correct orientation was confirmed by sequencing using the BgIb-intron-F sequencing primer (CTGGTCATCATCCTGCCTTT). T47D^M cells were transfected as described with CDK2-HA-encoding plasmids; 48 h later, cell lysates were prepared and immunoprecipitated using anti-HA-specific antibody overnight at 4°C end over end. The interaction of the CDK2-HA truncated proteins with PARP-1 was detected by Western blot using PARP-1-specific antibody.

Additional methods are provided in the Supplemental Material.

Acknowledgments

We thank Valerie Schreiber for the PARP-1-GST plasmid (pBChPARP-1), and Guillermo Vicent, Luciano Di Croce, and Juan Valcárcel for their critical reading of and advice on the manuscript. Proteomics analyses were performed in the CRG/UPF Proteomics Unit. The experimental work was supported by grants from the Departament d'Innovació Universitat i Empresa (DIUE), Ministerio de Educación y Ciencia (MEC) BMC 2003-02902, Consolider (CSD2006-00049), Fondo de Investigación Sanitaria (FIS) PI0411605 and CP04/00087, FEDER BIO2008-0205, and EU IP HEROIC. R.H.G.W. planned and performed experiments and helped with the writing of the manuscript. G.C. and D.S. performed microarray and ChIP-seq data analysis. J.B. performed all protein modeling simulations, analysis, and data interpretation in the laboratory of B.O. F.L.D. performed all immunofluorescence experiments and assisted in the planning and writing of the manuscript. J.F.M. performed the in vitro phosphorylation assays. CDK2 inhibitor microarrays were performed by C.B. A.S.N. performed ChIP experiments. B.O. performed all protein modeling simulations, analysis, and data interpretation. M.B. coordinated the project, planned the experiments, and wrote the manuscript. All authors discussed the results and commented on the manuscript.

References

- Aboul-Ela N, Jacobson EL, Jacobson MK. 1988. Labeling methods for the study of poly- and mono(ADP-ribose) metabolism in cultured cells. *Anal Biochem* **174**: 239–250.
- Adams PD, Sellers WR, Sharma SK, Wu AD, Nalin CM, Kaelin WG Jr. 1996. Identification of a cyclin-cdk2 recognition motif present in substrates and p21-like cyclin-dependent kinase inhibitors. *Mol Cell Biol* **16**: 6623–6633.
- Ame JC, Spelnhauer C, de Murcia G. 2004. The PARP superfamily. *Bioessays* **26**: 882–893.
- Chambon P, Weill JD, Mandel P. 1963. Nicotinamide mononucleotide activation of new DNA-dependent polyadenylic acid synthesizing nuclear enzyme. *Biochem Biophys Res Commun* **11**: 39–43.
- Cohen-Armon M, Visochek L, Rozensal D, Kalal A, Geistrikh I, Klein R, Bendetz-Nezer S, Yao Z, Seger R. 2007. DNA-independent PARP-1 activation by phosphorylated ERK2 increases Elk1 activity: A link to histone acetylation. *Mol Cell* **25**: 297–308.
- Dantzer F, de La Rubia G, Menissier-De Murcia J, Hostomsky Z, de Murcia G, Schreiber V. 2000. Base excision repair is impaired in mammalian cells lacking poly(ADP-ribose) polymerase-1. *Biochemistry* **39**: 7559–7569.
- Gagné JP, Moreel X, Gagné P, Labelle Y, Droit A, Chevalier-Paré M, Bourassa S, McDonald D, Hendzel MJ, Prigent C, et al. 2009. Proteomic investigation of phosphorylation sites in poly(ADP-ribose) polymerase-1 and poly(ADP-ribose) glycohydrolase. *J Proteome Res* **8**: 1014–29.
- Ghabreau L, Roux JP, Frappart PO, Mathevet P, Patricot LM, Mokni M, Korbi S, Wang ZQ, Tong WM, Frappart L. 2004. Poly(ADP-ribose) polymerase-1, a novel partner of progesterone receptors in endometrial cancer and its precursors. *Int J Cancer* **109**: 317–321.
- Hassa PO, Buerki C, Lombardi C, Imhof R, Hottiger MO. 2003. Transcriptional coactivation of nuclear factor- κ B-dependent gene expression by p300 is regulated by poly(ADP-ribose) polymerase-1. *J Biol Chem* **278**: 45145–45153.
- Inbar-Rozensal D, Castiel A, Visochek L, Castel D, Dantzer F, Izraeli S, Cohen-Armon M. 2009. A selective eradication of human nonhereditary breast cancer cells by phenanthridine-derived polyADP-ribose polymerase inhibitors. *Breast Cancer Res* **11**: R78. doi: 10.1186/bcr2445.
- Jacobson EL, Jacobson MK. 1976. Pyridine nucleotide levels as a function of growth in normal and transformed 3T3 cells. *Arch Biochem Biophys* **175**: 627–634.
- Ju BG, Rosenfeld MG. 2006. A breaking strategy for topoisomerase II β /PARP-1-dependent regulated transcription. *Cell Cycle* **5**: 2557–2560.
- Ju BG, Solum D, Song EJ, Lee KJ, Rose DW, Glass CK, Rosenfeld MG. 2004. Activating the PARP-1 sensor component of the groucho/TLE1 corepressor complex mediates a CaMKinase II δ -dependent neurogenic gene activation pathway. *Cell* **119**: 815–829.
- Ju BG, Lunyak VV, Perissi V, Garcia-Bassets I, Rose DW, Glass CK, Rosenfeld MG. 2006. A topoisomerase II β -mediated dsDNA break required for regulated transcription. *Science* **312**: 1798–1802.
- Kauppinen TM, Chan WY, Suh SW, Wiggins AK, Huang EJ, Swanson RA. 2006. Direct phosphorylation and regulation of poly(ADP-ribose) polymerase-1 by extracellular signal-regulated kinases 1/2. *Proc Natl Acad Sci* **103**: 7136–7141.
- Kim MY, Mauro S, Gevry N, Lis JT, Kraus WL. 2004. NAD⁺-dependent modulation of chromatin structure and transcription by nucleosome binding properties of PARP-1. *Cell* **119**: 803–814.

- Kraus WL, Lis JT. 2003. PARP goes transcription. *Cell* **113**: 677–683.
- Krishnakumar R, Gamble MJ, Frizzell KM, Berrocal JG, Kininis M, Kraus WL. 2008. Reciprocal binding of PARP-1 and histone H1 at promoters specifies transcriptional outcomes. *Science* **319**: 819–821.
- Lange CA. 2008. Integration of progesterone receptor action with rapid signaling events in breast cancer models. *J Steroid Biochem Mol Biol* **108**: 203–212.
- Lee KH, Benson DR, Kuczera K. 2000. Transitions from α to π helix observed in molecular dynamics simulations of synthetic peptides. *Biochemistry* **39**: 13737–13747.
- Luo X, Kraus WL. 2012. On PAR with PARP: Cellular stress signaling through poly(ADP-ribose) and PARP-1. *Genes Dev* **26**: 417–432.
- Masson M, Niedergang C, Schreiber V, Muller S, Menissier-de Murcia J, de Murcia G. 1998. XRCC1 is specifically associated with poly(ADP-ribose) polymerase and negatively regulates its activity following DNA damage. *Mol Cell Biol* **18**: 3563–3571.
- Mayya V, Lundgren DH, Hwang SI, Rezaul K, Wu L, Eng JK, Rodionov V, Han DK. 2009. Quantitative phosphoproteomic analysis of T cell receptor signaling reveals system-wide modulation of protein–protein interactions. *Sci Signal* **2**: ra46. doi: 10.1126/scisignal.2000007.
- Moore NL, Weigel NL. 2011. Regulation of progesterone receptor activity by cyclin dependent kinases 1 and 2 occurs in part by phosphorylation of the SRC-1 carboxyl-terminus. *Int J Biochem Cell Biol* **43**: 1157–1167.
- Narayanan R, Adigun AA, Edwards DP, Weigel NL. 2005. Cyclin-dependent kinase activity is required for progesterone receptor function: Novel role for cyclin A/Cdk2 as a progesterone receptor coactivator. *Mol Cell Biol* **25**: 264–277.
- Oei SL, Shi Y. 2001. Transcription factor Yin Yang 1 stimulates poly(ADP-ribosyl)ation and DNA repair. *Biochem Biophys Res Commun* **284**: 450–454.
- Parvi R, Lewis B, Kim TK, Dilworth FJ, Erdjument-Bromage H, Tempst P, de Murcia G, Evans R, Chambon P, Reinberg D. 2005. PARP-1 determines specificity in a retinoid signaling pathway via direct modulation of mediator. *Mol Cell* **18**: 83–96.
- Penning TD, Zhu GD, Gong J, Thomas S, Gandhi VB, Liu X, Shi Y, Klinghofer V, Johnson EF, Park CH, et al. 2005. Optimization of phenyl-substituted benzimidazole carboxamide poly(ADP-ribose) polymerase inhibitors: Identification of (S)-2-(2-fluoro-4-(pyrrolidin-2-yl)phenyl)-1H-benzimidazole-4-carboxamide (A-966492), a highly potent and efficacious inhibitor. *J Med Chem* **53**: 3142–3153.
- Poirier GG, de Murcia G, Jongstra-Bilen J, Niedergang C, Mandel P. 1982. Poly(ADP-ribosyl)ation of polynucleosomes causes relaxation of chromatin structure. *Proc Natl Acad Sci* **79**: 3423–3427.
- Sartorius CA, Takimoto GS, Richer JK, Tung L, Horwitz KB. 2000. Association of the Ku autoantigen/DNA-dependent protein kinase holoenzyme and poly(ADP-ribose) polymerase with the DNA binding domain of progesterone receptors. *J Mol Endocrinol* **24**: 165–182.
- Schreiber V, Ame JC, Dolle P, Schultz I, Rinaldi B, Fraulob V, Menissier-de Murcia J, de Murcia G. 2002. Poly(ADP-ribose) polymerase-2 (PARP-2) is required for efficient base excision DNA repair in association with PARP-1 and XRCC1. *J Biol Chem* **277**: 23028–23036.
- Slattery E, Dignam JD, Matsui T, Roeder RG. 1983. Purification and analysis of a factor which suppresses nick-induced transcription by RNA polymerase II and its identity with poly (ADP-ribose) polymerase. *J Biol Chem* **258**: 5955–5959.
- Truss M, Bartsch J, Schelbert A, Hache RJ, Beato M. 1995. Hormone induces binding of receptors and transcription factors to a rearranged nucleosome on the MMTV promoter in vivo. *EMBO J* **14**: 1737–1751.
- Tulin A, Stewart D, Spradling AC. 2002. The *Drosophila* heterochromatic gene encoding poly(ADP-ribose) polymerase (PARP) is required to modulate chromatin structure during development. *Genes Dev* **16**: 2108–2119.
- Vicent GP, Nacht AS, Font-Mateu J, Castellano G, Gaveglia L, Ballare C, Beato M. 2011. Four enzymes cooperate to displace histone H1 during the first minute of hormonal gene activation. *Genes Dev* **25**: 845–862.